Coronary vasomotor dysfunction in cancer survivors treated with thoracic irradiation

John D. Groarke, MBBCh, MPH,[a] Sanjay Divakaran, MD,[a,b]
Anju Nohria, MD,[a] Joseph H. Killoran, PhD,[c] Sharmila Dorbala, MD, MPH,[b]
Ruth M. Dunne, MBBCh, MPH,[b] Jon Hainer, BS,[b]
Viviany R. Taqueti, MD, MPH,[b] Ron Blankstein, MD,[a,b]
Harvey J. Mamon, MD, PhD,[c] and Marcelo F. Di Carli, MD[a,b]

[a] Cardiovascular Division, Department of Medicine, Brigham and Women's Hospital, Harvard Medical School, Boston, MA
[b] Cardiovascular Imaging Program, Departments of Medicine and Radiology, Brigham and Women's Hospital, Harvard Medical School, Boston, MA
[c] Department of Radiation Oncology, Brigham and Women's Hospital, Harvard Medical School, Boston, MA

Received Nov 19, 2019; Revised May 22, 2020; accepted Jun 11, 2020
doi:10.1007/s12350-020-02255-5

Background. **We sought to test the hypothesis that thoracic radiation therapy (RT) is associated with impaired myocardial flow reserve (MFR), a measure of coronary vasomotor dysfunction.**

Methods. **We retrospectively studied thirty-five consecutive patients (71% female, mean ± standard deviation (SD) age: 66 ± 11 years) referred clinically for positron emission tomography/computed tomography (PET/CT) myocardial perfusion imaging at a median (interquartile range, IQR) interval of 4.3 (2.1, 9.7) years following RT for a variety of malignancies. Radiation dose-volume histograms were generated for the heart and coronary arteries for each patient.**

Results. **The median (IQR) of mean cardiac radiation doses was 12.0 (1.2, 24.2) Gray. There were significant inverse correlations between mean radiation dose and global MFR (MFR_{Global}) and MFR in the left anterior descending artery territory (MFR_{LAD}): Pearson's correlation coefficient = − .37 (*P* = .03) and − .38 (*P* = .03), respectively. For every one Gray increase in mean cardiac radiation dose, there was a mean ± standard error decrease of .02 ± .01 in MFR_{Global} (*P* = .04) and MFR_{LAD} (*P* = .03) after adjustment.**

Electronic supplementary material The online version of this article (https://doi.org/10.1007/s12350-020-02255-5) contains supplementary material, which is available to authorized users.

The authors of this article have provided a PowerPoint file, available for download at SpringerLink, which summarizes the contents of the paper and is free for re-use at meetings and presentations. Search for the article DOI on SpringerLink.com.

All editorial decisions for this article, including selection of reviewers and the final decision, were made by guest editor Saurabh Malhotra, MD, MPH.

Funding This work was supported by the Goodman Master Clinician Award, Brigham and Women's Hospital, Boston, MA granted to Dr. John Groarke. Dr. Divakaran is supported by grant number T32 HL094301 from the National Heart, Lung, and Blood Institute. Dr. Dorbala is supported by grant number R01 HL130563 from the National Heart, Lung, andBlood Institute. Dr. Taqueti is supported by grant number K23HL135438 from the National Heart, Lung, and Blood Institute. Dr. Di Carli is supported by grant number R01 HL132021 from the National Heart, Lung, and Blood Institute.

John D. Groarke and Sanjay Divakaran have contributed equally to this work and serve as joint first authors.

Reprint requests: Marcelo F. Di Carli, MD, Cardiovascular Imaging Program, Departments of Medicine and Radiology, Brigham and Women's Hospital, Harvard Medical School, Boston, MA; *mdicarli@bwh.harvard.edu*

1071-3581/$34.00

Conclusions. **In patients with a history of RT clinically referred for cardiac stress PET, we found an inverse correlation between mean cardiac radiation dose and coronary vasomotor function. (J Nucl Cardiol 2021;28:2976–87.)**

Key Words: Microvascular dysfunction • PET • myocardial blood flow • atherosclerosis • MPI

Abbreviations

CAD	Coronary artery disease
CT	Computed tomography
IHD	Ischemic heart disease
LAD	Left anterior descending artery
LCx	Left circumflex coronary artery
MFR	Myocardial flow reserve
PET	Positron emission tomography
RCA	Right coronary artery
RT	Radiation therapy

See related editorial, pp. 2988–2991

INTRODUCTION

Improved survival among cancer patients is compromised by increased cardiovascular morbidity and mortality associated with thoracic radiation therapy (RT) for thoracic malignancies, such as breast cancer, Hodgkin lymphoma (HL), and non-small cell lung cancer.[1–7] A proportion of this excess cardiovascular mortality is related to the significantly increased risk of coronary artery disease (CAD) and coronary revascularization in survivors of thoracic irradiation.[2,8] This predisposition to CAD following RT appears to be mediated by radiation-induced macrovascular and microvascular injury. Microvascular pathology is characterized by damage to vascular endothelial cells and a decrease in capillary density,[9] leading to reduced vascular reserve, myocardial ischemia, myocyte death and progressive fibrosis.[10,11] Radiation-induced macrovascular injury manifests as accelerated development of atherosclerosis. This atherosclerosis demonstrates similar morphology to, and shares common pathogenic pathways, with atherosclerosis driven by genetic and risk factors unrelated to radiation.[11,12] As such, synergistic interaction between radiation-induced effects and other independent pathogenic effects that expedite age-related atherosclerosis is likely.[10]

Radiation-induced heart disease was initially regarded as a ''deterministic'' adverse effect of radiation that only occurred when cardiac radiation dose exceeded a defined threshold.[12] However, increasing data support a stochastic and linear dose-dependent relationship between radiation dose and risk of ischemic heart disease (IHD), with no apparent threshold dose.[2,13–15] Myocardial flow reserve (MFR), defined as the ratio of myocardial blood flow at peak stress to that at rest, is a measure of coronary large and small vessel function that can be non-invasively assessed using positron emission tomography (PET). Impaired MFR predicts major adverse cardiovascular events in patients with and without flow-limiting CAD,[16–19] as well as cardiovascular events among patients with known or suspected CAD,[20,21] diabetes mellitus,[22] renal dysfunction,[23] and obesity.[24] Given the diffuse nature of radiation injury, MFR (which incorporates the effects of epicardial CAD, diffuse atherosclerosis, vessel remodeling, and microvascular dysfunction[25]) may be a useful indicator of radiation-induced coronary injury. The relationship between cardiac radiation dose and MFR has not been investigated. This study was designed to test the hypothesis that RT is associated with impaired MFR in a dose-dependent manner.

MATERIALS AND METHODS

Study population

A retrospective cross-sectional study was designed. Thirty-five patients referred for PET/computed tomography (CT) myocardial perfusion imaging from 2007 to 2013 at Brigham and Women's Hospital (Boston, MA) who had a prior history of RT were identified using ICD-9 codes. The presence of cancer diagnosis, as well as history of RT were confirmed by medical chart review. A variety of cancer diagnoses were included in this study to provide an adequate range of cardiac radiation doses to evaluate the dose–response relationship with MFR. Demographic factors, cardiovascular symptoms, medications, and risk factors were determined at the time of PET imaging by a structured patient interview and medical chart review. The presence of cardiovascular risk factors pre-RT was also assessed by medical chart review, and pre-RT chest CT imaging was reviewed (where available) for the presence of coronary artery calcium. A Morise clinical risk score at the time of PET imaging was calculated for all patients which considers age, sex, symptoms, tobacco use, hyperlipidemia, diabetes mellitus, hypertension, estrogen status, body mass index (BMI), and family history of CAD to assess the pre-test probability of CAD.[26] Oncological histories, including details of RT, were obtained from medical chart review. We also constructed a control group (without a history of RT) to compare MFR values with the study cohort via 1:1 matching by age, sex, the absence or presence of known IHD, and Morise score. The Partners HealthCare Institutional Review Board approved the study and waived the need for informed consent.

Positron emission tomography imaging

Patients were imaged with a whole-body PET/CT scanner (Discovery RX or STE LightSpeed 64, GE Healthcare, Milwaukee, WI) following an overnight fast. After CT-based transmission imaging used for attenuation correction, 2D listmode images were acquired at rest for 430 s and formatted into a dynamic sequence of a total of 27 frames (14 × 5 s, 6 × 10 s, 3 × 20 s, 3 × 30 s, and 1 × 150 s) for Rubidium-82 PET (N = 33) or 20 min and formatted into a dynamic sequence of a total of 34 frames (12 × 5 s, 6 × 10 s, 6 × 30 s, 5 × 60 s, and 5 × 120 s for N13-ammonia (N = 2). Maximal coronary hyperemia was then achieved using a standard intravenous infusion of regadenoson (N = 24, 68.6%), dipyridamole (N = 5, 14.2%), adenosine (N = 3, 8.6%), or dobutamine (N = 3, 8.6%). At peak stress, the second dose of the same tracer was injected, and images were recorded in the same manner. Symptoms, hemodynamic parameters, and 12-lead electrocardiography were monitored and recorded during pharmacological stress. All PET images were reconstructed with ordered subsets expectation maximization (OSEM) algorithm with two iterations and 23 subsets. All physics corrections including detector sensitivity normalization, attenuation, dead time, randoms, and scatter were applied. Post-smoothing 3D Butterworh filter was also applied with cutoff = 4 and order = 1. Matrix size of the PET images was 128 × 128 × 47 with a voxel size of 3.27 × 3.27 × 3.27 mm^3. Prompt gamma rays with 776 keV of Rubidium-82 were not corrected since the effect of these gammas in image quantitation is negligible in 2D PET imaging.[27]

Image analysis

Semi-quantitative analysis of myocardial perfusion Rest and stress perfusion images were interpreted by experienced observers using the standard 17-segment model and 5-point scoring system for semi-quantitative visual analysis.[28] The summed rest and stress scores were calculated as the sum of the rest and stress scores for all segments, respectively. The summed difference score (SDS) was calculated as the difference between summed stress and summed rest scores. Summed rest score and SDS scores were converted into percent myocardium scar and ischemia, respectively, by dividing the corresponding summed score by the maximum possible score of 68 and multiplying by 10. Extent of ischemia was categorized as normal (≤ 3%), mild ischemia (3-7%), moderate ischemia (7-10%), and severe ischemia (> 10%).[29]

In addition, a visual assessment of calcification[30] of the thoracic aorta, pericardium, coronary arteries, and heart valves using attenuation correction CT scans was performed for all patients. Review of the lung parenchyma for radiation-induced effects was not done due to inadequate image quality for this purpose.

Gated myocardial perfusion positron emission tomography images Left ventricular volumes and ejection fraction were calculated from gated myocardial perfusion PET images at rest and stress for each patient using commercially available software (INVIA, Corridor 4-DM, Ann Arbor, Michigan).

Myocardial blood flow and flow reserve quantification Absolute rest and peak stress myocardial blood flow (MBF, in mL/min/g of tissue) were computed from the dynamic stress and rest imaging series using commercially available software (Corridor4DM; Ann Arbor, MI), as previously described.[31,32] Regional and global MBF were calculated by fitting the arterial blood and tissue time-activity curves to a two-compartment tracer kinetic model, as previously described.[31,32] Per-patient MFR was calculated as the ratio of maximal MBF at peak stress over that at rest for each vascular territory and the entire left ventricle. The intra-class correlation coefficient for MFR computation among multiple readers in our laboratory is .94 (95% CI .88-.98), indicating excellent reproducibility.

Quantification of radiation dosimetry

Three-dimensional CT-based treatment planning data were available for 31 (88.6%) patients. The heart and coronary arteries were contoured using a treatment planning system (Aria Eclipse Treatment Planning System, Varian Medical Systems, Inc., CA, USA). The heart contour included the atria, ventricles and blood volume within the cardiac chambers. The cranial limit of the heart excluded the pulmonary trunk, ascending aorta and superior vena cava. The caudal limit of the heart was the inferior myocardial border. The left main coronary artery was included with the left anterior descending coronary artery (LAD). The left circumflex coronary artery (LCx) was contoured from its origin at the point of bifurcation of the left main coronary artery. The right coronary artery (RCA) was contoured from its origin off the aortic root. Each coronary artery was contoured from its origin down to the last visible segment of the vessel. Dose-volume histograms were generated for the heart, LAD, LCx, and RCA for each patient (Figure 1).

Three-dimensional dose-volume exposures were unavailable for four of the patients (11.4%). These four patients were treated for Hodgkin lymphoma 19.4 ± 10.6 years prior to PET/CT imaging. Planning parameters including prescription, isocenter location, and field sizes obtained from treatment records and two-dimensional planning images for these patients were used to reconstruct individual radiation plans using thoracic CT images imported into the treatment planning system. Dose-volume histograms were then generated for contoured heart and coronary arteries similar to above.

Statistical analysis

Continuous, normally distributed variables are presented as mean ± standard deviation (SD). Continuous, non-normal data are presented as median with interquartile range (IQR). Categorical variables are presented as percentages. The

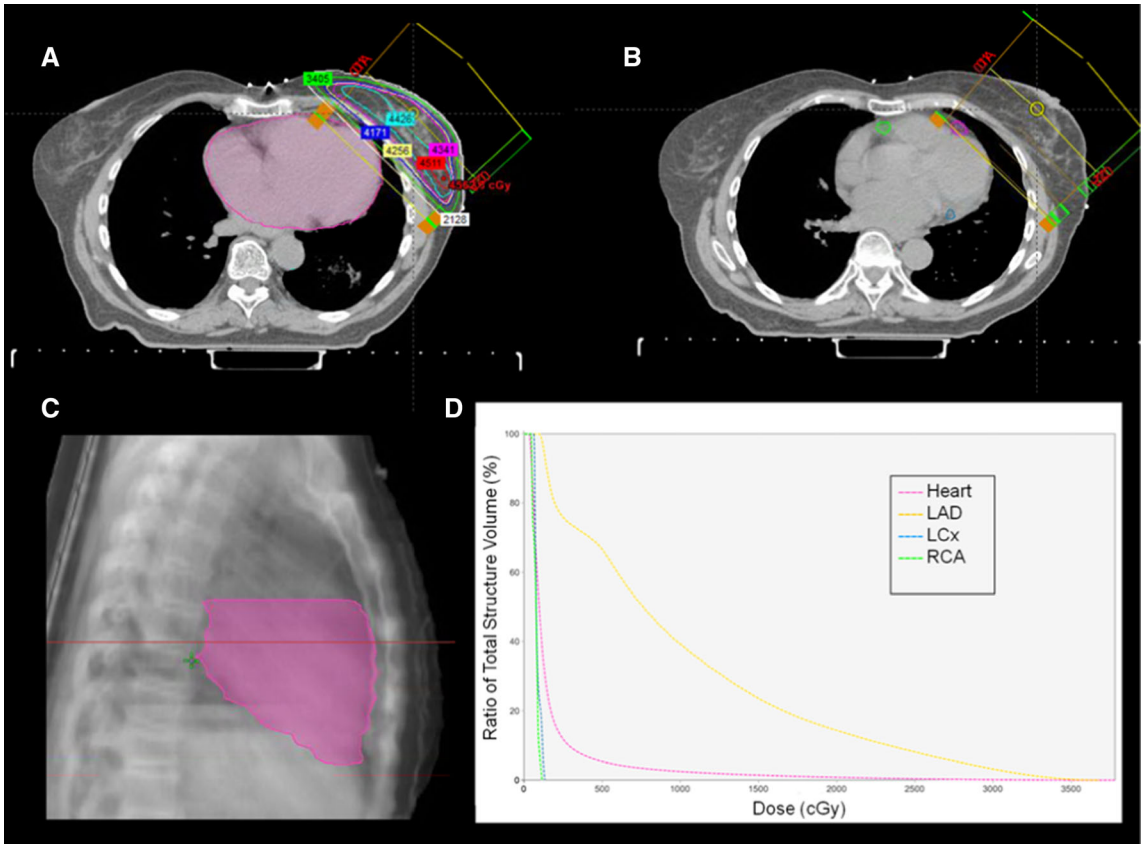

Figure 1. Radiation plan for left breast irradiation in a 77-year-old female following breast conserving surgery for left breast cancer. A total dose of 4256 cGy was delivered in 16 fractions (266 cGy per fraction) over 22 days. (**A**) The heart is contoured (pink) using treatment planning software. (**B**) Left anterior descending artery (pink), right coronary artery (green), and left circumflex artery (blue) contours are outlined. (**C**) The contoured heart volume is outlined on this sagittal tomograph. (**D**) Dose-volume histogram with the ratio of total structure volume (%) plotted against radiation dose (cGy) for the entire heart volume and individual coronary arteries. *LAD*, left anterior descending; *LCx*, left circumflex; *RCA*, right coronary artery.

relationship between global or territorial MFR with mean cardiac radiation dose was assessed using Pearson's correlation coefficient. Simple linear regression was used to determine the change in global and territorial MFR per unit change in mean cardiac radiation dose. Multivariable linear regression was used to assess the association of global and territorial MFR with mean cardiac radiation dose after adjusting for Morise clinical risk score, semi-quantitative measures of ischemia, and duration of interval from RT to PET/CT. To assess for potential bias introduced by IHD on the association between MFR and radiation dose, analyses were repeated censoring all patients with a history of IHD. All statistical analyses were performed using SAS version 9.3 (SAS Institute, Cary, North Carolina, USA). Two-tailed P values of $< .05$ were considered significant, and a P value between .05 and .10 was considered as a trend toward significance.

RESULTS

The majority of patients were female (N = 25, 71.4%) with a mean age of 66.0 ± 10.6 years (Table 1). Cardiovascular comorbidities such as increased BMI (N = 30, 85.7%), hyperlipidemia (N = 26, 74.3%), and hypertension (N = 22, 62.9%) were prevalent in this cohort. Six patients (17.1%) had diabetes. Of the 26 patients with hyperlipidemia, 22 patients with hypertension, and six with diabetes at the time of PET imaging, seven, two, and zero developed the respective risk factor between RT and PET imaging. Six (17.1%) patients had a history of IHD prior to PET (four (11.4%) of the six had a history of IHD prior to RT). Twenty-one of the twenty-nine (82.9%) IHD naïve patients had a Morise score of $\geq$ 9 indicating an intermediate (N = 19) or high (N = 2) pre-test probability of CAD. Forty percent

Table 1. Baseline characteristics of entire patient cohort (N = 35) including radiation oncology history

Age, years	66.0 ± 10.6
Female, N (%)	25 (71.4%)
Cardiovascular risk factors	
Hypertension, N (%)	22 (62.9%)
Dyslipidemia, N (%)	26 (74.3%)
Diabetes mellitus, N (%)	6 (17.1%)
Family history of IHD, N (%)	3 (8.6%)
Smoking history, N (%)	2 (5.7%)
BMI > 25 kg/m^2, N (%)	30 (85.7%)
Ischemic heart disease, N (%)	6 (17.1%)
Congestive heart failure, N (%)	12 (34.3%)
LVEF at rest, %	56.8 ± 13.9%
Morise score	9.9 ± 2.7
Cardiovascular medications	
Aspirin, N (%)	19 (54.3%)
Lipid lowering agents, N (%)	25 (71.4%)
Beta-blockers, N (%)	22 (62.9%)
Calcium channel blockers, N (%)	6 (17.1%)
Nitrates, N (%)	3 (8.6%)
Diuretics, N (%)	12 (34.3%)
Oral hypoglycemic agents/insulin, N (%)	6 (17.1%)
Indication for PET/CT MPI	
Chest pain, N (%)	4 (11.4%)
Dyspnea, N (%)	14 (40.0%)
Arrhythmia, N (%)	4 (11.4%)
CHF evaluation, N (%)	2 (5.7%)
Other, N (%)	11 (31.5%)
Radiation oncology history	
Age at RT, years	58.8 ± 14.0 years
Interval from RT to PET, years	4.3 (2.1, 9.7) years
Mean radiation dose to heart, Gy	12.0 (1.2, 24.2)
Mean radiation dose to LAD, Gy	8.6 (1.6, 14.0)
Mean radiation dose to LCx, Gy	12.0 (.8, 20.4)
Mean radiation dose to RCA, Gy	12.0 (1.1, 27.3)
Adjuvant chemotherapy, N (%)	27 (77.1%)
Indication for RT	
Esophageal cancer, N (%)	7 (20.0%)
Left breast cancer, N (%)	6 (17.1%)
Right breast cancer, N (%)	6 (17.1%)
Lung cancer, N (%)	5 (14.3%)
Pre-BMT conditioning, N (%)	5 (14.3%)
Hodgkin's lymphoma, N (%)	4 (11.5%)
Other, N (%)	2 (5.7%)

BMI, body mass index; *BMT*, bone marrow transplant; *CHF*, congestive heart failure; *IHD*, ischemic heart disease; *LAD*, left anterior descending; *LCx*, left circumflex; *LVEF*, left ventricular ejection fraction; *MPI*, myocardial perfusion imaging; *PET/CT*, positron emission tomography/computed tomography; *RCA*, right coronary artery; *RT*, radiation therapy

(N = 14) of patients were referred for PET/CT myocardial perfusion imaging for clinical evaluation of dyspnea (Table 1).

The median interval from RT to PET/CT imaging was 4.3 (2.1, 9.7) years. The median cardiac radiation dose was 12.0 (1.2, 24.2) Gy, and 27 patients (77.1%) received adjuvant anthracycline chemotherapy for treatment of their malignancy. Indications for RT are outlined in Table 1.

Imaging parameters

The median percent of myocardial ischemia for the entire cohort was 0 (0, 1)%: 26 patients (74.3%) had no ischemia, three (8.6%) had mild ischemia, two (5.7%) had moderate ischemia, and four (11.4%) had evidence of severe ischemia. There was no association between percent of myocardial ischemia and mean cardiac radiation dose (P = .90). Global MFR was less than 2.00 in 18 (51.4%) patients, and median global MFR in the overall cohort was 2.00 (1.53, 2.41) (Table 2). The frequency of MFR < 2.00 was similar across the three coronary artery territories (P = .45).

Attenuation correction computed tomography findings

Coronary artery calcification was identified on the attenuation correction CT images of 19 patients (54.3%). Thirteen of these patients had chest CTs available for review pre-RT, and 12 of the 13 had coronary artery calcification present pre-RT. Atherosclerotic calcification was identified in the aortic root, visualized ascending aorta, and visualized descending aorta of 40.0%, 14.3%, and 60.0% of patients, respectively. Mitral annular calcification was present in four (11.4%) patients (Figure 2). Pericardial calcification was absent in all patients, and mean pericardial thickness was within normal range (2.3 ± .5 mm).

Myocardial flow reserve and cardiac radiation dose

Mean global MFR (MFR_{Global}) in the study cohort (1.98) was significantly lower than in a control group (2.28) formed via 1:1 matching by age, sex, the absence or presence of IHD, and Morise score (P = .047) (Table 3). MFR_{Global} and MFR in the LAD territory (MFR_{LAD}) demonstrated significant negative linear correlations with mean cardiac radiation dose (r = − .37, P = .03 and r = − .38, P = .03, respectively) (Figure 3). There was no significant correlation between mean cardiac radiation dose and MFR in the RCA territory (MFR_{RCA}) (r = − .30, P = .08) or between

Table 2. Imaging parameters for entire patient cohort (N = 35)

Left ventricular scar, %	0 (0, 0) %
Left ventricular ischemia, %	0 (0, 1)%
LAD territory ischemia, %	0 (0, 1)%
LCx territory ischemia, %	0 (0, 1)%
RCA territory ischemia, %	0 (0, 0)%
LV ejection fraction at rest, %	56.8 ± 13.9
LV ejection fraction at stress, %	60.2 ± 14.9
Global myocardial blood flow (rest), mL g^{-1} min^{-1} (median IQR)	1.05 (.87, 1.39)
Global myocardial blood flow (stress), mL g^{-1} min^{-1} (median, IQR)	2.12 (1.67, 2.72)
Global myocardial flow reserve (MFR_{Global}) (median, IQR)	2.00 (1.53, 2.41)
Median MFR_{LAD} (median, IQR)	1.93 (1.46, 2.19)
Median MFR_{LCx} (median, IQR)	1.97 (1.63, 2.42)
Median MFR_{RCA} (median, IQR)	2.08 (1.67, 2.42)
LAD calcification	
None/mild/moderate/severe, N (%)	17 (48.6%)/4 (11.4%)/7 (20.0%)/7 (20.0%)
LCx calcification	
None/mild/moderate/severe, N (%)	23 (65.7%)/5 (14.3%)/4 (11.4%)/3 (8.6%)
RCA calcification	
None/mild/moderate/severe, N (%)	22 (62.9%)/6 (17.1%)/4 (11.4%)/3 (8.6%)
Aortic root calcification	
None/mild/moderate/severe, N (%)	21 (60.0%)/9 (25.7%)/2 (5.7%)/3 (8.6%)
Ascending aorta calcification	
None/mild/moderate/severe, N (%)	30 (85.7%)/5 (14.3%)/0 (0%)/0 (0%)
Descending aorta calcification	
None/mild/moderate/severe, N (%)	14 (40.0%)/11 (31.4%)/8 (22.9%)/2 (5.7%)
Mitral annular calcification, N (%)	4 (11.4%)
Aortic valve calcification, N (%)	1 (2.9%)
Pericardial calcification, N (%)	0 (0%)
Pericardial thickness, mm	2.3 ± .5 mm

IQR, interquartile range; *LAD*, left anterior descending; *LCx*, left circumflex; *LV*, left ventricular; *RCA*, right coronary artery

mean cardiac radiation dose and MFR in the LCx territory (MFR_{LCx}) ($r = -.29$, $P = .11$) (Figure 3).

Compared with mean cardiac radiation dose, MFR_{LAD} demonstrated an even stronger negative linear correlation with mean radiation dose to the LAD ($r = -.50$, $P = .002$). There was no significant correlation between MFR_{LCx} and mean radiation dose to the LCx ($r = -.31$, $P = .07$) or between MFR_{RCA} and mean radiation dose to the RCA ($r = -.21$, $P = .22$).

In unadjusted analyses, every one Gy increase in mean cardiac radiation dose was associated with a .02 ± .01 decrease in MFR_{Global} ($P = .03$) and MFR_{LAD} ($P = .03$). Similarly, these associations remained significant after adjusting for Morise score, SDS, and duration of interval from RT to PET/CT imaging (Table 4). There was a trend toward a similar .02 ± .01 decrease in MFR_{RCA} per one Gy increase in cardiac mean radiation dose in unadjusted ($P = .08$) and adjusted ($P = .07$) analyses. No significant associations were observed for MFR_{LCx}.

Ischemic heart disease naïve cohort After excluding patients with known IHD (N = 6), MFR_{Global} and MFR_{LAD} demonstrated significant negative linear correlations with mean cardiac radiation dose ($r = -.41$ ($P = .03$) and $r = -.45$ ($P = .02$), respectively) in the remaining 29 patients. MFR_{LCx} and MFR_{RCA} did not demonstrate significant correlations with mean cardiac radiation dose ($P = .09$ and $P = .15$, respectively). A

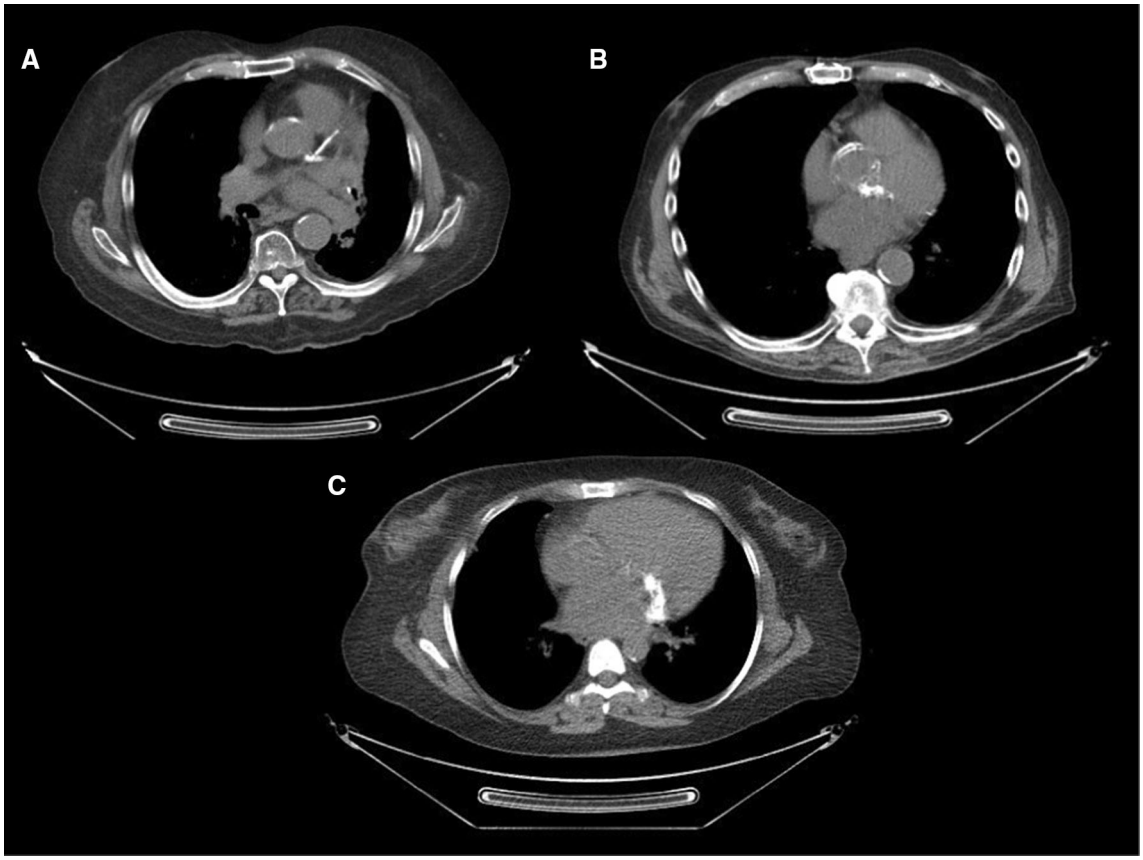

Figure 2. Attenuation correction computed tomography axial images from three patients with prior thoracic irradiation undergoing positron emission tomography/computed tomography myocardial perfusion imaging. (**A**) Extensive atherosclerotic calcification of left main artery, and proximal left anterior descending and left circumflex arteries, in addition to calcification of the aortic root and descending thoracic aorta. (**B**) Extensive atherosclerotic calcification of the aortic root is evident on this ungated attenuation correction computed tomography axial image. (**C**) Prominent mitral annular calcification is present.

Table 3. Comparison of myocardial flow reserve with a matched control group

	RT patients (N = 35)	Control patients (N = 35)	*P* value
Age, years	66.0 ± 10.6	65.5 ± 10.3	.85
Female, N (%)	25 (71.4%)	25 (71.4%)	1.00
Ischemic heart disease, N (%)	6 (17.1%)	6 (17.1%)	1.00
Morise score	9.9 ± 2.7	9.9 ± 2.6	.96
Mean global myocardial flow reserve	1.98 ± .56	2.28 ± .69	.047

To compare global myocardial flow reserve in the study cohort with individuals without a history of thoracic irradiation therapy, a control group was formed via 1:1 matching on age, sex, the absence or presence of ischemic heart disease, and Morise score. *RT*, radiation therapy.

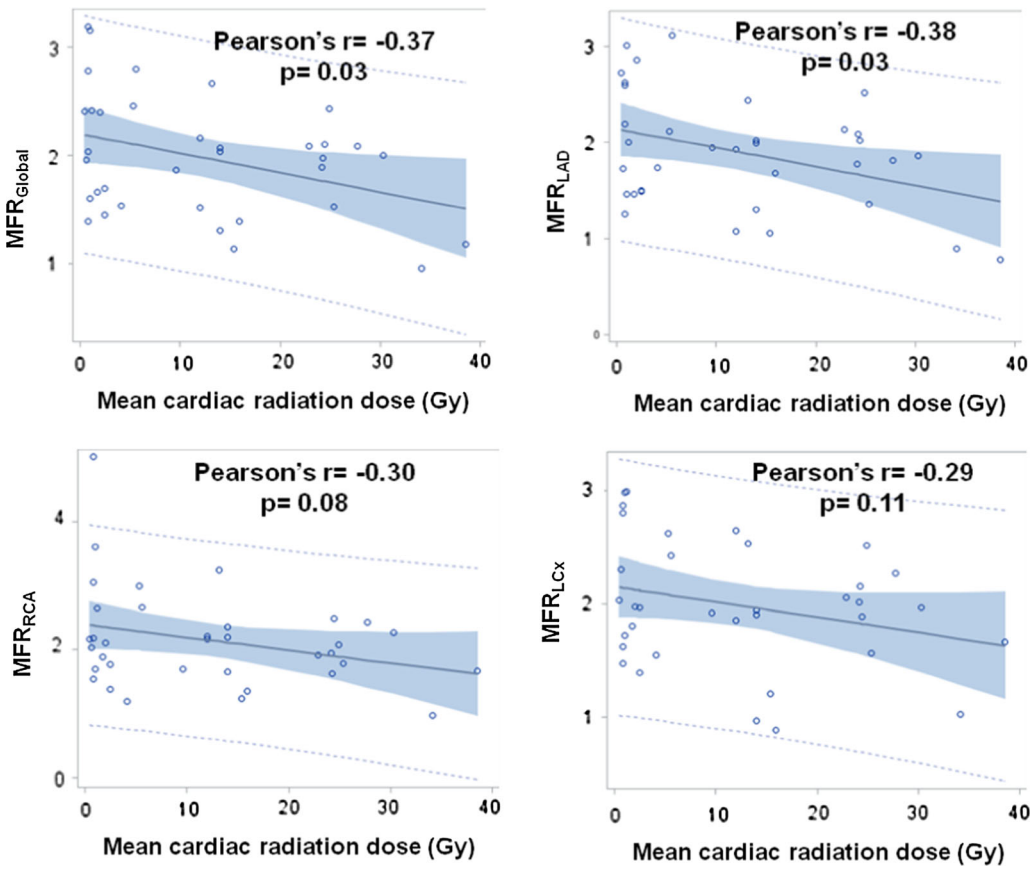

Figure 3. Relationship of global and territorial myocardial flow reserve to mean cardiac radiation dose. *LAD*, left anterior descending; *LCx*, left circumflex; *MFR*, myocardial flow reserve; *RCA*, right coronary artery.

decrease of .02 ± .01 in MFR_{Global} and MFR_{LAD} was observed for every one Gy increase in mean cardiac radiation dose among IHD naïve patients in unadjusted (P = .03 and P = .02, respectively) analyses and after adjusting for Morise score, SDS, and interval from RT to PET/CT imaging (P = .03 and .02, respectively) (Table 4). No such significant associations were observed for MFR_{LCx} or MFR_{RCA}.

DISCUSSION

Mean MFR_{Global} was significantly lower in survivors of thoracic irradiation referred for PET/CT myocardial perfusion imaging when compared with a matched control group. MFR_{Global} and MFR_{LAD} demonstrated significant negative correlations with mean cardiac radiation in survivors of thoracic irradiation. These negative correlations remain significant after adjusting for semi-quantitative measures of ischemia, Morise clinical risk score, interval from RT to PET/CT imaging, and presence of IHD. No such correlation with mean cardiac radiation dose was demonstrated for MFR or percent ischemia in other coronary territories. The lack of significance in the LCx and RCA territories may have been due to insufficient power related to small sample size.

Radiation therapy can damage blood vessels of any size, including the microcirculation.[33] Endothelial cell injury and reduced capillary density that characterize radiation-mediated microvascular pathology reduce coronary vascular reserve and predispose to myocardial ischemia.[9,10,34] The exact mechanisms that contribute to impaired MFR, and similarly to increased risk of IHD, cannot be determined from this study but are likely multifactorial in this patient cohort. Radiation-induced endothelial dysfunction of the microcirculation together with radiation injury to the cardiac sympathetic nerve fibers may, in part, explain the association between radiation dose and impaired MFR. Furthermore, radiation exposure is associated with chronic, subclinical, low-grade inflammation as evidenced by persistent increases in inflammatory cytokines and biomarkers,[35]

Table 4. Unadjusted and adjusted change in myocardial flow reserve per Gray increase in mean cardiac radiation dose for all patients and for patients with no known ischemic heart disease

	Unadjusted mean ± SE change in MFR per Gray increase in mean cardiac radiation dose		Adjusted mean ± SE change in MFR per Gray increase in mean cardiac radiation dose	
Entire cohort (N = 35)				
MFR_{Global}	− .018 ± .008	*P* = .03	− .018 ± .008	*P* = .04
MFR_{LAD}	− .020 ± .008	*P* = .03	− .020 ± .009	*P* = .03
MFR_{LCx}	− .014 ± .008	*P* = .11	− .013 ± .008	*P* = .11
MFR_{RCA}	− .020 ± .011	*P* = .08	− .021 ± .011	*P* = .07
Patients with no history of IHD (N = 29)				
MFR_{Global}	− .019 ± .008	*P* = .03	− .020 ± .009	*P* = .03
MFR_{LAD}	− .023 ± .009	*P* = .02	− .023 ± .009	*P* = .02
MFR_{LCx}	− .014 ± .008	*P* = .09	− .013 ± .008	*P* = .11
MFR_{RCA}	− .019 ± .012	*P* = .15	− .020 ± .013	*P* = .13

IHD, ischemic heart disease; *LAD*, left anterior descending; *LCx*, left circumflex; *MFR*, myocardial flow reserve; *RCA*, right coronary artery; *SE*, standard error

which in turn affects coronary microvascular function as evidenced by impaired MFR.[36] In addition, the role of inflammation in initiation, progression, and rupture of atherosclerotic lesions is well established.[37] Therefore, increased risk of CAD following RT may also be, in part, related to direct vessel injury, persistent low-grade inflammation, or a synergistic interaction of the two. MFR could potentially play a role in identifying radiation survivors who would most benefit from anti-inflammatory therapies, and in monitoring treatment response in clinical trials.[25]

The dose-dependent relationship between mean cardiac radiation dose and MFR observed in this study is in keeping with the radiation dose–response relationship observed for cardiovascular mortality, non-cancer mortality, and/or major coronary events with no apparent threshold.[2,13,38,39] Although advances in radiation techniques have achieved a reduction in the risk of IHD associated with RT over time,[40] the risk of CAD associated with newer radiation techniques remains poorly quantified.[33] Increased cardiovascular risk has been observed in patients with radiation doses to the heart as low as less than five Gy.[2,39,41] Therefore, even patients with low-dose radiation exposure to the heart may still require cardiovascular surveillance.

Non-invasive stress testing for CAD detection is advocated by consensus statements in asymptomatic patients five to ten years after radiation exposure, but the method of testing is not specified.[42] MFR quantification with PET/CT myocardial perfusion imaging may offer incremental risk stratification of patients following thoracic irradiation beyond conventional risk factors.[18] For patients without known CAD undergoing PET/CT myocardial perfusion imaging, CT coronary artery calcium scoring can be performed simultaneously. These data may be used to detect subclinical CAD and provide an opportunity to alter cardiovascular morbidity. Moreover, useful information pertaining to radiation-induced cardiovascular sequelae can be obtained from careful review of the low-dose CT acquired on all patients for attenuation correction. For example, atherosclerotic calcification of the coronary arteries and thoracic aorta were prevalent on the attenuation correction CTs in this patient cohort.

Finally, recent data have been published implicating coronary microvascular dysfunction in the development of heart failure, particularly heart failure with preserved ejection fraction.[43] As more data emerge regarding the link between RT and the development of heart failure,[44] more research is needed to investigate if coronary microvascular dysfunction is on the causal pathway between RT and heart failure.

Study limitations

The sample size of this study is small, and these results require validation through larger studies. This is a single center, retrospective study and patients were clinically referred for PET/CT myocardial perfusion imaging, which may introduce selection bias. This bias is likely reflected in the high prevalence of cardiovascular risk factors among this cohort. Nevertheless, cardiovascular disease is common among cancer survivors. Two PET/CT systems, two tracers, and four

pharmacologic stress agents were used. Given the retrospective nature of the study, pre-RT PET/CT myocardial perfusion imaging was not available to study MFR prior to RT for the study cohort. This is an important limitation as the presence and/or degree of pre-existing coronary vasomotor dysfunction is not known for the patients in this study. To mitigate this limitation, we included a control group matched for age, sex and clinical risk and found that MFR was reduced in the study cohort compared to controls, suggesting that exposure to radiation may affect coronary vasomotor function. Three-dimensional dose-volume exposures were unavailable for four (11.4%) patients and three-dimensional model reconstructions of historical treatment plans of these patients were used to determine individual organ doses. Such reconstructions are subject to geometric uncertainties that predispose to dose discrepancies, but likely reconstruct organ exposures in a more patient specific manner than phantom-based alternative methods.[45] Contouring of target volumes for the coronary arteries did not include side branches, and thus, mean radiation doses to these coronary arteries were likely underestimated. Similarly, the MFR for a coronary artery territory represents the mean MFR across all myocardial segments supplied by that coronary artery. Thus, focusing on radiation dose delivered to the main epicardial coronary artery may be an insufficient proxy for radiation dose delivered to the epicardial vessel, branch vessels, and microvasculature that supply the myocardial segments. Prospective studies are necessary to determine if medical therapy for patients treated with RT with impaired MFR in the absence of overt ischemia is associated with improved outcomes.

CONCLUSION

MFR_{Global} and MFR_{LAD} demonstrated a significant negative correlation with mean cardiac radiation dose in survivors of thoracic malignancies treated with RT. This inverse relationship was independent of IHD, ischemia, cardiovascular clinical risk score, or interval from RT. This observation is supported by the dose–response relationship with risk of cardiovascular morbidity and mortality following RT demonstrated in multiple prior studies. Continued efforts to minimize incidental cardiac exposure during RT for adjacent malignancies are warranted and the benefits of cardiovascular surveillance with risk modification should be evaluated. PET/CT myocardial perfusion imaging is an informative strategy for non-invasive functional stress testing recommended for this patient cohort. Further studies are needed to prospectively study the effect of RT on MFR, as well as the effect of medical therapy on outcomes in patients with impaired MFR after RT, to expand on this hypothesis generating work.

NEW KNOWLEDGE GAINED

A significant inverse correlation between mean cardiac radiation dose and coronary vasomotor function is evident in survivors of malignancies treated with thoracic RT.

Disclosures

Dr. Groarke receives research support from Amgen, Inc. Dr. Nohria receives research support from Amgen, Inc. and consulting fees from Takeda Oncology. Dr. Dorbala is a member of an advisory board for Proclara, Pfizer, and General Electric Health Care, and receives grant support from Pfizer. Dr. Blankstein receives research support from Amgen Inc. and Astellas Inc. Dr. Di Carli has received consulting fees from Sanofi and General Electric, and research grants from Gilead Sciences and Spectrum Dynamics. All other authors have reported that they have no relationships relevant to the contents of this paper to disclose.

References

1. Clarke M, Collins R, Darby S, Davies C, Elphinstone P, Evans E, et al. Effects of radiotherapy and of differences in the extent of surgery for early breast cancer on local recurrence and 15-year survival: An overview of the randomised trials. Lancet 2005;366:2087-106.
2. Darby SC, Ewertz M, McGale P, Bennet AM, Blom-Goldman U, Bronnum D, et al. Risk of ischemic heart disease in women after radiotherapy for breast cancer. N Engl J Med 2013;368:987-98.
3. Rehammar JC, Jensen MB, McGale P, Lorenzen EL, Taylor C, Darby SC, et al. Risk of heart disease in relation to radiotherapy and chemotherapy with anthracyclines among 19,464 breast cancer patients in Denmark, 1977-2005. Radiother Oncol 2017;123:299-305.
4. Henson KE, Reulen RC, Winter DL, Bright CJ, Fidler MM, Frobisher C, et al. Cardiac mortality Among 200 000 five-year survivors of cancer diagnosed at 15 to 39 years of age: The teenage and young adult cancer survivor study. Circulation 2016;134:1519-31.
5. Speirs CK, DeWees TA, Rehman S, Molotievschi A, Velez MA, Mullen D, et al. Heart dose is an independent dosimetric predictor of overall survival in locally advanced non-small cell lung cancer. J Thorac Oncol 2017;12:293-301.
6. Dess RT, Sun Y, Matuszak MM, Sun G, Soni PD, Bazzi L, et al. Cardiac events after radiation therapy: Combined analysis of prospective multicenter trials for locally advanced non-small-cell lung cancer. J Clin Oncol 2017;35:1395-402.
7. Atkins KM, Rawal B, Chaunzwa TL, Lamba N, Bitterman DS, Williams CL, et al. Cardiac radiation dose, cardiac disease, and mortality in patients with lung cancer. J Am Coll Cardiol 2019;73:2976-87.
8. Galper SL, Yu JB, Mauch PM, Strasser JF, Silver B, Lacasce A, et al. Clinically significant cardiac disease in patients with Hodgkin lymphoma treated with mediastinal irradiation. Blood 2011;117:412-8.

9. Stewart FA, Hoving S, Russell NS. Vascular damage as an underlying mechanism of cardiac and cerebral toxicity in irradiated cancer patients. Radiat Res 2010;174:865-9.
10. Lancellotti P, Nkomo VT, Badano LP, Bergler-Klein J, Bogaert J, Davin L, et al. Expert consensus for multi-modality imaging evaluation of cardiovascular complications of radiotherapy in adults: A report from the European Association of Cardiovascular Imaging and the American Society of Echocardiography. Eur Heart J Cardiovasc Imaging 2013;14:721-40.
11. Darby SC, Cutter DJ, Boerma M, Constine LS, Fajardo LF, Kodama K, et al. Radiation-related heart disease: Current knowledge and future prospects. Int J Radiat Oncol Biol Phys 2010;76:656-65.
12. Schultz-Hector S, Trott KR. Radiation-induced cardiovascular diseases: Is the epidemiologic evidence compatible with the radiobiologic data? Int J Radiat Oncol Biol Phys 2007;67:10-8.
13. van Nimwegen FA, Schaapveld M, Cutter DJ, Janus CP, Krol AD, Hauptmann M, et al. Radiation dose-response relationship for risk of coronary heart disease in survivors of Hodgkin lymphoma. J Clin Oncol 2016;34:235-43.
14. Jacobse JN, Duane FK, Boekel NB, Schaapveld M, Hauptmann M, Hooning MJ et al. Radiation dose-response for risk of myocardial infarction in breast cancer survivors. Int J Radiat Oncol Biol Phys 2018.
15. van den Bogaard VA, Ta BD, van der Schaaf A, Bouma AB, Middag AM, Bantema-Joppe EJ, et al. Validation and modification of a prediction model for acute cardiac events in patients with breast cancer treated with radiotherapy based on three-dimensional dose distributions to cardiac substructures. J Clin Oncol 2017;35:1171-8.
16. Ziadi MC, Dekemp RA, Williams KA, Guo A, Chow BJ, Renaud JM, et al. Impaired myocardial flow reserve on rubidium-82 positron emission tomography imaging predicts adverse outcomes in patients assessed for myocardial ischemia. J Am Coll Cardiol 2011;58:740-8.
17. Herzog BA, Husmann L, Valenta I, Gaemperli O, Siegrist PT, Tay FM, et al. Long-term prognostic value of 13 N-ammonia myocardial perfusion positron emission tomography added value of coronary flow reserve. J Am Coll Cardiol 2009;54:150-6.
18. Naya M, Murthy VL, Foster CR, Gaber M, Klein J, Hainer J, et al. Prognostic interplay of coronary artery calcification and underlying vascular dysfunction in patients with suspected coronary artery disease. J Am Coll Cardiol 2013;61:2098-106.
19. Taqueti VR, Everett BM, Murthy VL, Gaber M, Foster CR, Hainer J, et al. Interaction of impaired coronary flow reserve and cardiomyocyte injury on adverse cardiovascular outcomes in patients without overt coronary artery disease. Circulation 2015;131:528-35.
20. Murthy VL, Naya M, Foster CR, Hainer J, Gaber M, Di Carli G, et al. Improved cardiac risk assessment with noninvasive measures of coronary flow reserve. Circulation 2011;124:2215-24.
21. Taqueti VR, Hachamovitch R, Murthy VL, Naya M, Foster CR, Hainer J, et al. Global coronary flow reserve is associated with adverse cardiovascular events independently of luminal angiographic severity and modifies the effect of early revascularization. Circulation 2015;131:19-27.
22. Murthy VL, Naya M, Foster CR, Gaber M, Hainer J, Klein J, et al. Association between coronary vascular dysfunction and cardiac mortality in patients with and without diabetes mellitus. Circulation 2012;126:1858-68.
23. Murthy VL, Naya M, Foster CR, Hainer J, Gaber M, Dorbala S, et al. Coronary vascular dysfunction and prognosis in patients with chronic kidney disease. JACC Cardiovasc imaging 2012;5:1025-34.
24. Bajaj NS, Osborne MT, Gupta A, Tavakkoli A, Bravo PE, Vita T, et al. Coronary microvascular dysfunction and cardiovascular risk in obese patients. J Am Coll Cardiol 2018;72:707-17.
25. Taqueti VR, Ridker PM. Inflammation, coronary flow reserve, and microvascular dysfunction: Moving beyond cardiac syndrome X. JACC Cardiovasc Imaging 2013;6:668-71.
26. Morise AP. Comparison of the Diamond-Forrester method and a new score to estimate the pretest probability of coronary disease before exercise testing. Am Heart J 1999;138:740-5.
27. Moncayo VM, Garcia EV. Prompt-gamma compensation in Rb-82 myocardial perfusion 3D PET/CT: Effect on clinical practice. J Nucl Cardiol 2018;25:606-8.
28. Schelbert HR, Beanlands R, Bengel F, Knuuti J, Dicarli M, Machac J, et al. PET myocardial perfusion and glucose metabolism imaging: Part 2-Guidelines for interpretation and reporting. J Nucl Cardiol 2003;10:557-71.
29. Leslie WD, Tully SA, Yogendran MS, Ward LM, Nour KA, Metge CJ. Prognostic value of automated quantification of 99mTc-sestamibi myocardial perfusion imaging. J Nucl Med 2005;46:204-11.
30. Chiles C, Duan F, Gladish GW, Ravenel JG, Baginski SG, Snyder BS, et al. Association of coronary artery calcification and mortality in the national lung screening trial: A comparison of three scoring methods. Radiology 2015;276:82-90.
31. El Fakhri G, Sitek A, Guérin B, Kijewski MF, Di Carli MF, Moore SC. Quantitative dynamic cardiac 82Rb PET using generalized factor and compartment analyses. J Nucl Med 2005;46:1264-71.
32. El Fakhri G, Kardan A, Sitek A, Dorbala S, Abi-Hatem N, Lahoud Y, et al. Reproducibility and accuracy of quantitative myocardial blood flow assessment with (82)Rb PET: Comparison with (13)N-ammonia PET. J Nucl Med 2009;50:1062-71.
33. Gaya AM, Ashford RF. Cardiac complications of radiation therapy. Clin Oncol (R Coll Radiol) 2005;17:153-9.
34. Schultz-Hector S. Radiation-induced heart disease: Review of experimental data on dose response and pathogenesis. Int J Radiat Biol 1992;61:149-60.
35. Hayashi T, Kusunoki Y, Hakoda M, Morishita Y, Kubo Y, Maki M, et al. Radiation dose-dependent increases in inflammatory response markers in A-bomb survivors. Int J Radiat Biol 2003;79:129-36.
36. Recio-Mayoral A, Rimoldi OE, Camici PG, Kaski JC. Inflammation and microvascular dysfunction in cardiac syndrome X patients without conventional risk factors for coronary artery disease. JACC Cardiovascular imaging 2013;6:660-7.
37. Ridker PM, Luscher TF. Anti-inflammatory therapies for cardiovascular disease. Eur Heart J 2014.
38. Preston DL, Shimizu Y, Pierce DA, Suyama A, Mabuchi K. Studies of mortality of atomic bomb survivors. Report 13: Solid cancer and noncancer disease mortality: 1950-1997 2003. Radiation research 2012;178:AV146-72.
39. Carr ZA, Land CE, Kleinerman RA, Weinstock RW, Stovall M, Griem ML, et al. Coronary heart disease after radiotherapy for peptic ulcer disease. Int J Radiat Oncol Biol Phys 2005;61:842-50.
40. Giordano SH, Kuo YF, Freeman JL, Buchholz TA, Hortobagyi GN, Goodwin JS. Risk of cardiac death after adjuvant radiotherapy for breast cancer. J Natl Cancer Inst 2005;97:419-24.
41. Azizova TV, Muirhead CR, Druzhinina MB, Grigoryeva ES, Vlasenko EV, Sumina MV, et al. Cardiovascular diseases in the cohort of workers first employed at Mayak PA in 1948-1958. Radiat Res 2010;174:155-68.
42. Zamorano JL, Lancellotti P, Rodriguez Muñoz D, Aboyans V, Asteggiano R, Galderisi M, et al 2016 ESC Position Paper on cancer treatments and cardiovascular toxicity developed under the auspices of the ESC Committee for Practice Guidelines: The Task

Force for cancer treatments and cardiovascular toxicity of the European Society of Cardiology (ESC). Eur Heart J 2016;37:2768-801.

43. Taqueti VR, Solomon SD, Shah AM, Desai AS, Groarke JD, Osborne MT, et al. Coronary microvascular dysfunction and future risk of heart failure with preserved ejection fraction. Eur Heart J 2018;39:840-9.
44. van Nimwegen FA, Ntentas G, Darby SC, Schaapveld M, Hauptmann M, Lugtenburg PJ, et al. Risk of heart failure in survivors of Hodgkin lymphoma: Effects of cardiac exposure to radiation and anthracyclines. Blood 2017;129:2257-65.
45. Ng A, Brock KK, Sharpe MB, Moseley JL, Craig T, Hodgson DC. Individualized 3D reconstruction of normal tissue dose for patients with long-term follow-up: A step toward understanding dose risk for late toxicity. Int J Radiat Oncol Biol Phys 2012;84:e557-63.